

Electronic Supplementary Material (ESI) for Chemical Communications.
This journal is © The Royal Society of Chemistry 2021

Supporting Information for:

RBD conjugate vaccine with built-in TLR1/2 agonist is highly immunogenic against SARS-CoV-2 and variants of concern

Shi-Hao Zhou, Ru-Yan Zhang, Hai-Wei Zhang, Yan-Ling Liu, Yu Wen, Jian Wang, Yu-Ting Li, Zi-Wei You, Xu-Guang Yin, Hong Qiu, Rui Gong*, Guang-Fu Yang* and Jun Guo*

This file includes:

Materials and Synthetic Methods
Evaluation of Vaccine Candidates
Biological Testing Methods
Supplemental Schemes S1 to S3
Supplemental Table S1
Supplemental Fig. S1 to S12

Contents:

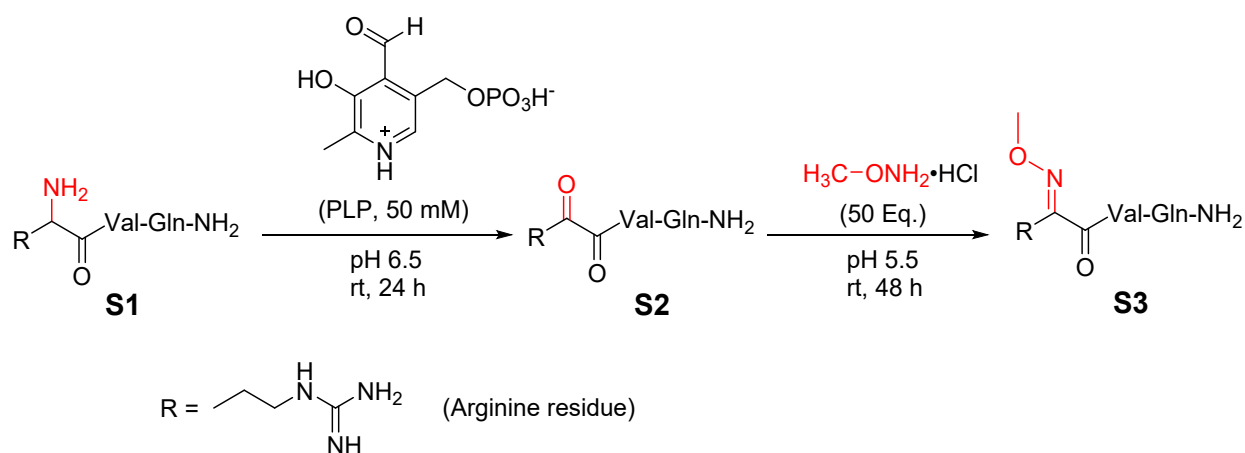
1. Materials and synthetic methods	S3
1.1 Materials	S3
1.2 Transamination and oxime formation reactions of model molecules	S3
1.3 Synthesis of the Pam ₃ CSK ₄ -Spacer-ONH ₂	S6
1.4 Synthesis of the Pam ₃ CSK ₄ -RBD	S9
2. Evaluation of vaccine candidates	S9
2.1 Vaccination formulation.....	S9
2.2 Characterization of vaccines	S10
2.3 Immunological evaluation	S10
3. Biological testing methods	S12
3.1 Culture and stimulation of RAW264.7 cells	S12
3.2 Immunization of mice and ELISA	S13
3.3 Enzyme-linked immunospot (ELISpot) assay.....	S13
3.4 Intracellular cytokine staining (ICS)	S14
3.5 Culture of ACE2-HEK293 cells and flow cytometry analysis.....	S14
3.6 Pseudovirus and live SARS-CoV-2 neutralization assay	S14
3.7 Statistical analysis and references	S15

1. Materials and synthetic methods

1.1 Materials

Recombinant RBD protein of SARS-CoV-2 (Arg319-Phe541, 223 amino acids, no Tag) was purchased from Sino Biological (40592-VNAH). All L-amino acids and resins were obtained from GL Biochem (Shanghai). Anhydrous dichloromethane (DCM) was obtained from the drying solvent system (passed through CaH₂) and can be used without further drying. The purchased anhydrous dimethylformamide (DMF) was stored on the active molecular sieves (4Å). 1,2-Distearoyl-sn-glycero-3-phosphocholine (DSPC) and cholesterol were purchased from TCI (Japan) and Energy Chemical (Shanghai, China), respectively. Pyridoxal 5'-Phosphate (PLP) was purchased from bidepharm (Shanghai, China). Pam₃CSK₄ and Fmoc-Pam₂Cys-OH were prepared by our group as previously described.^{1,2} InjectTM Alum adjuvant was purchased from Thermo Scientific. Peroxidase-conjugated Affinipure goat anti-mouse kappa antibody IgG, IgM were purchased from Jackson Immuno Research. Peroxidase-conjugated Affinipure goat anti-mouse kappa IgG1, IgG2a, IgG2b and IgG3 antibodies were purchased from Southern Biotechnology. Female BALB/c mice (age 6-8 weeks) were purchased and bred in the Laboratory Animal Centre of Huazhong Agriculture University. All animal experiments were approved by the Ethics Review Committee for Life Science Study of Central China Normal University and experimental animal care guidelines were adhered to. The HPLC was performed on Agilent 1260 infinity II prime LC system. The HRMS was performed on Bruker Compact TOF mass spectrometer by ESI and the MALDI-TOF-MS was performed on an AB SCIEX 5800 spectrometer.

1.2 Transamination and oxime formation reactions of model molecules



Scheme S1. Transamination and oxime formation reactions of model tripeptide (RBD₃₁₉₋₃₂₁, Arg-Val-Gln-NH₂).

To evaluate the yield of this coupling strategy, we synthesized an *N*-terminal fragment of the RBD protein (319-321, Arg-Val-Gln), which was conjugated to alkoxyamine through PLP-mediated transamination (See Scheme S1). The model peptide Arg-Val-Gln was synthesized by Fmoc solid-phase peptide synthesis (Rink amide resin). The Pyridoxal 5'-Phosphate (PLP) and tripeptide were mixed to achieve a final concentration of 1 mM tripeptide and 50 mM PLP at room temperature in PBS (pH=6.5) for 24 h. The reaction was assessed using ESI-MS and HPLC (210 nm, column: Agilent ZORBAX SB-C18, 250 × 9.2 mm, 5 μm, gradient: 2 mL/min, H₂O/Acetonitrile + 0.1% TFA, 0 min (95 : 5) → 15 min (70 : 30), 15 min). The ESI-MS showed that S1 transformed almost completely to S2, meanwhile no MS signals of PLP adducts were observed. Then the keto-RBD and alkoxyamine were mixed at room temperature (pH=5.5). In this step, we found that S2 transformed almost completely to S3. Hence, the coupling reaction of RBD peptide through PLP-mediated transamination was an efficient chemical reaction and basically completed.

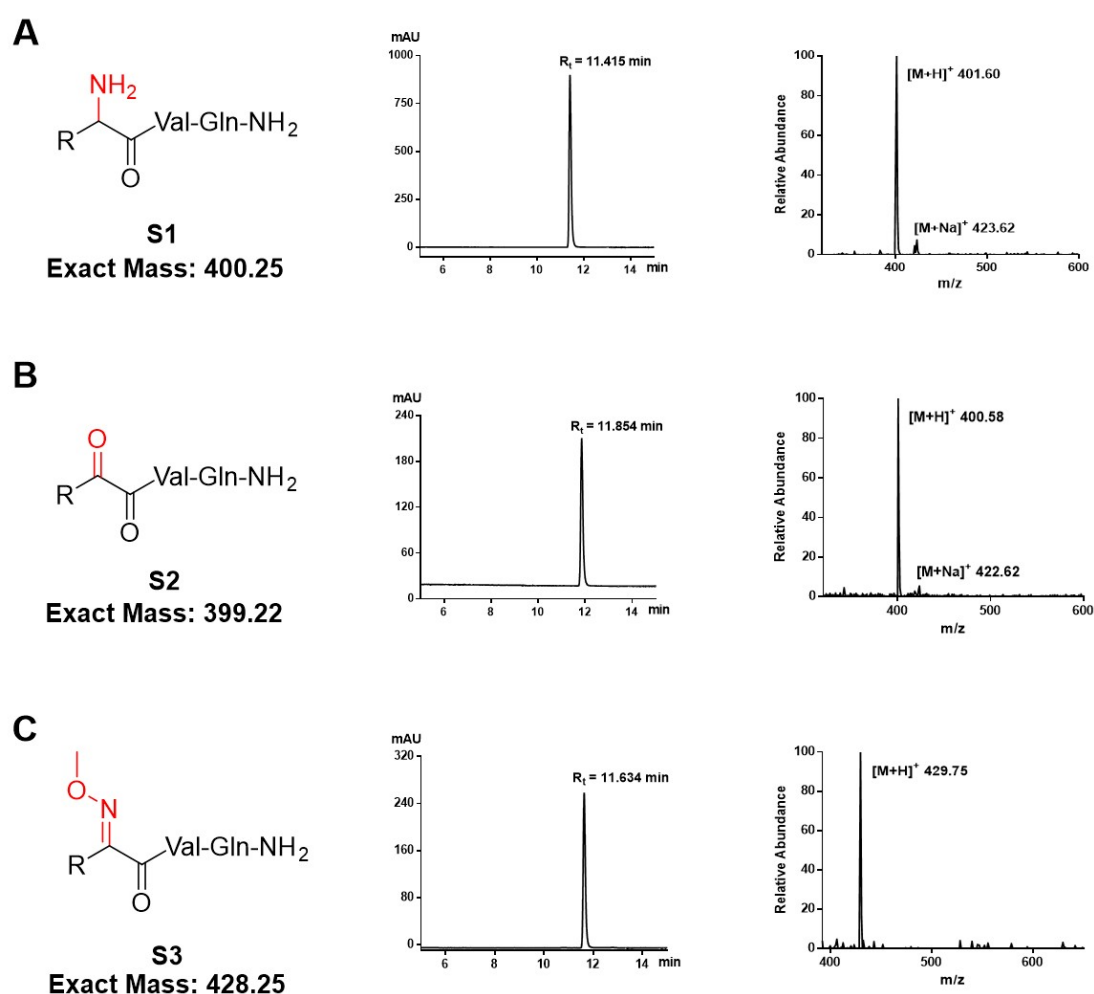
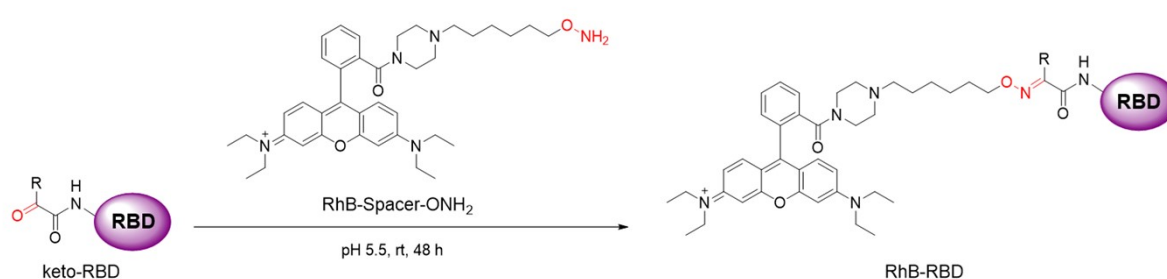


Fig. S1. Analytical HPLC (210 nm) and ESI-MS spectrum of compound S1 (A), S2 (B) and S3 (C). The reaction route can be referred to Scheme S1. The results showed that the coupling reaction of model tripeptide through PLP-mediated transamination was efficient and basically completed.



Scheme S2. RhB-Spacer-OH₂ was conjugated to keto-RBD through oxime formation reaction. The synthesis method of keto-RBD can be referred to Fig. 1.

In order to better verify the reaction yield, RhB-Spacer-OH₂ was prepared³ and conjugated to keto-RBD through oxime formation reaction (See Scheme S2). The reaction was assessed using HPLC (210 nm and 554 nm, column: Agilent ZORBAX 300SB-CN, 250 × 4.6 mm, 5 μm, gradient: 1 mL/min, H₂O/Acetonitrile + 0.1% TFA, 0 min (80 : 20) → 20 min (40 : 60), 20 min). The characteristic absorption peak of RhB at 554 nm showed that RhB was conjugated to RBD protein (Fig. S2). After transamination and oxime formation reactions, the total yield was more than 80%. In addition, SDS-page analysis also showed that RhB was conjugated to RBD protein (Fig. S3).

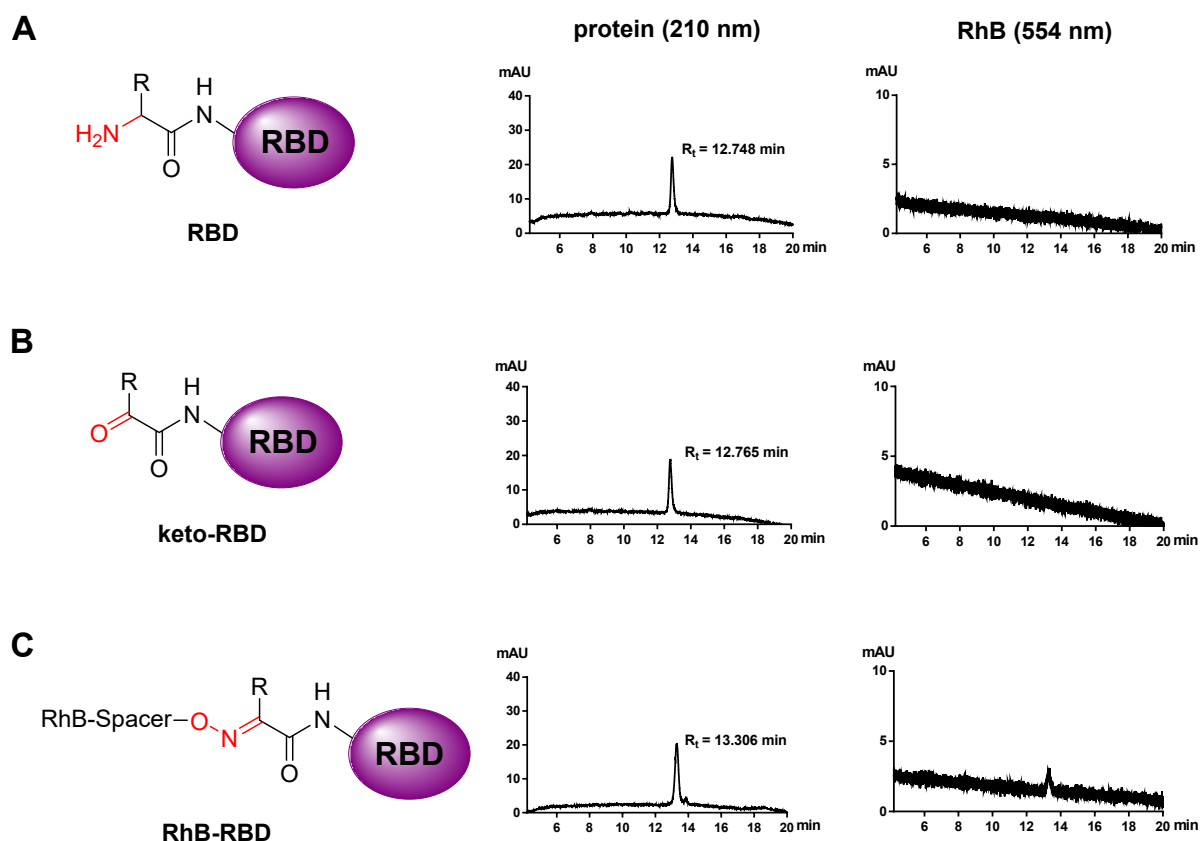


Fig. S2. HPLC spectrum (210 nm for protein and 554 nm for RhB) of RBD (A), keto-RBD (B), and RhB-RBD (C). The reaction route can be referred to Scheme S2. The characteristic absorption peak of RhB at 554 nm indicated that RhB was conjugated to RBD protein.

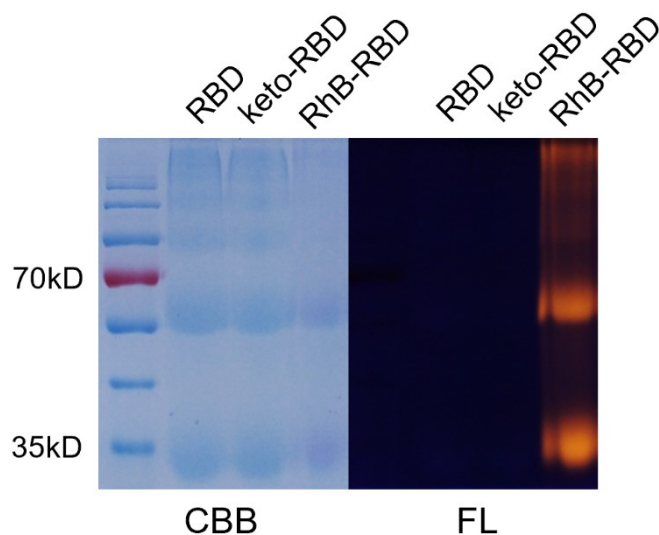
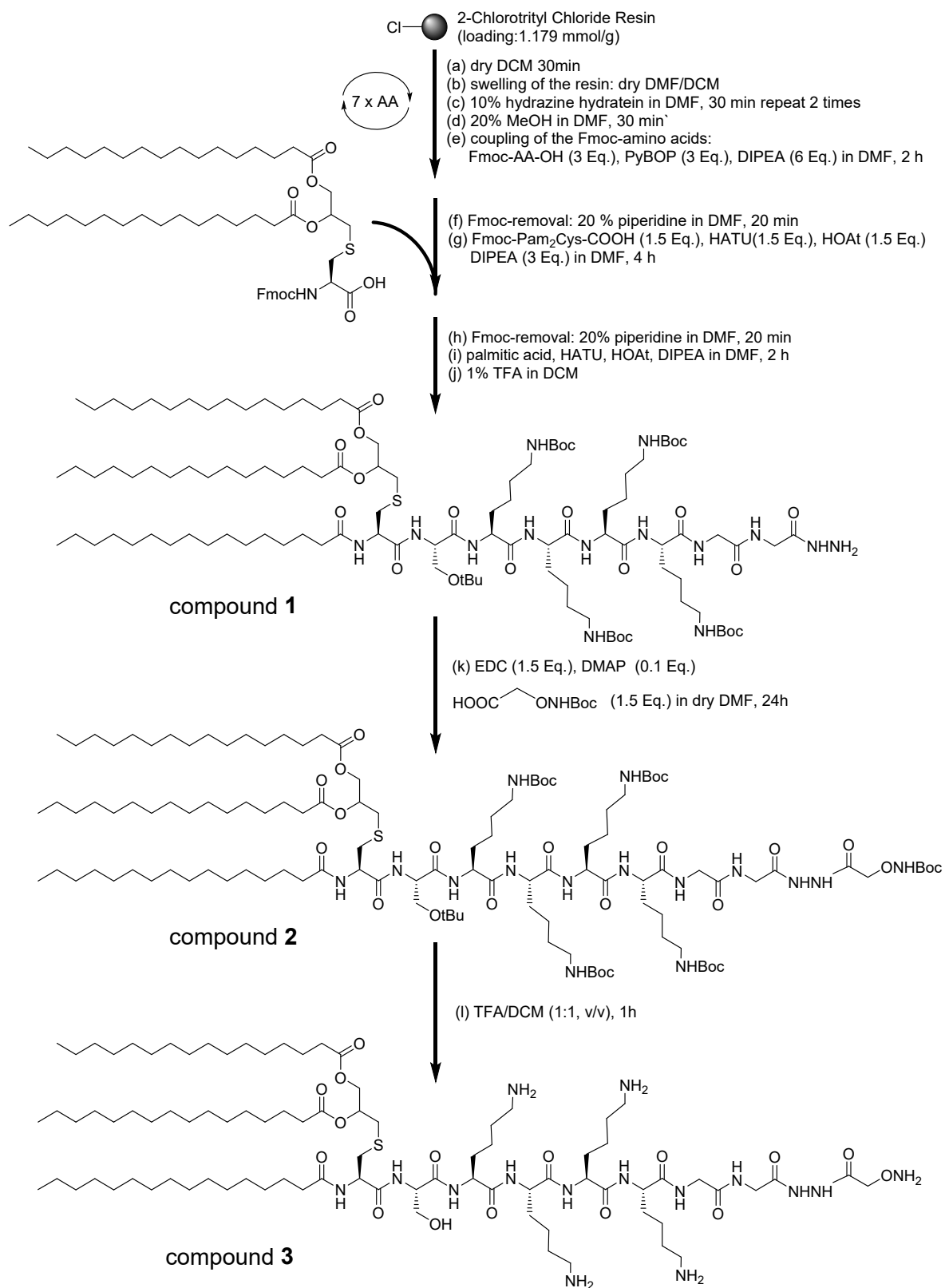


Fig. S3. SDS-PAGE analysis of RBD, keto-RBD and RhB-RBD. CBB and FL, indicating coomassie brilliant blue staining and in-gel fluorescent scanning, respectively. In-gel fluorescent scanning also showed that RhB was conjugated to RBD protein.

1.3 Synthesis of the Pam₃CSK₄-Spacer-OH₂

First, the synthesis of compound **1** was achieved according to Solid Phase Peptide Synthesis (see Scheme S1). After coupling of the (Boc-aminoxy) acetic acid, the purification of compound **2** by gel-filtration column chromatography Sephadex LH-20 (1:1, DCM-MeOH) gave compound **2** in 40% yields. Then the Pam₃CSK₄-Spacer-OH₂ (compound **3**) was obtained after removal of the side-chain protection. Finally, the Pam₃CSK₄-Spacer-OH₂ was purified by HPLC (210 nm, column: Agilent ZORBAX SB-CN, 4.6 × 250 mm, 5-Micron, gradient: 1 mL/min, H₂O/Acetonitrile + 0.1% TFA, 0 min (50 : 50) → 20 min (0 : 100), 20 min. Rt=11.599 min. The total yield was 17%). HRMS: Calcd for C₈₇H₁₆₇N₁₅O₁₆S [M+2H]²⁺ m/z=856.1291, [M+3H]³⁺ m/z=571.0885; found: 856.1281 [M+2H]²⁺; 571.0894 [M+3H]³⁺. ESI-MS: Calcd for C₈₇H₁₆₇N₁₅O₁₆S [M+H+Na]²⁺ m/z=867.12; found: 867.62 [M+H+Na]²⁺ (see Fig. S4).



Scheme S3. The synthesis route and the preparation method of Pam₃CSK₄-Spacer-ONH₂.

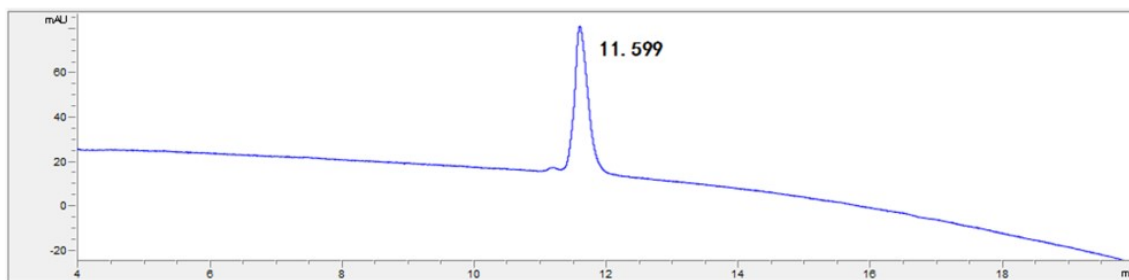
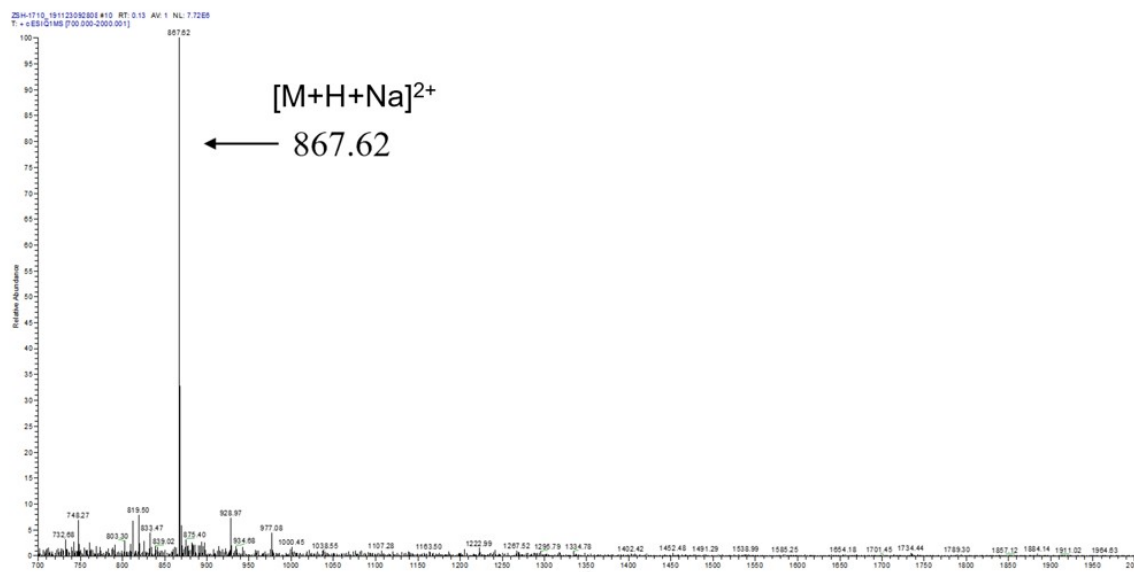
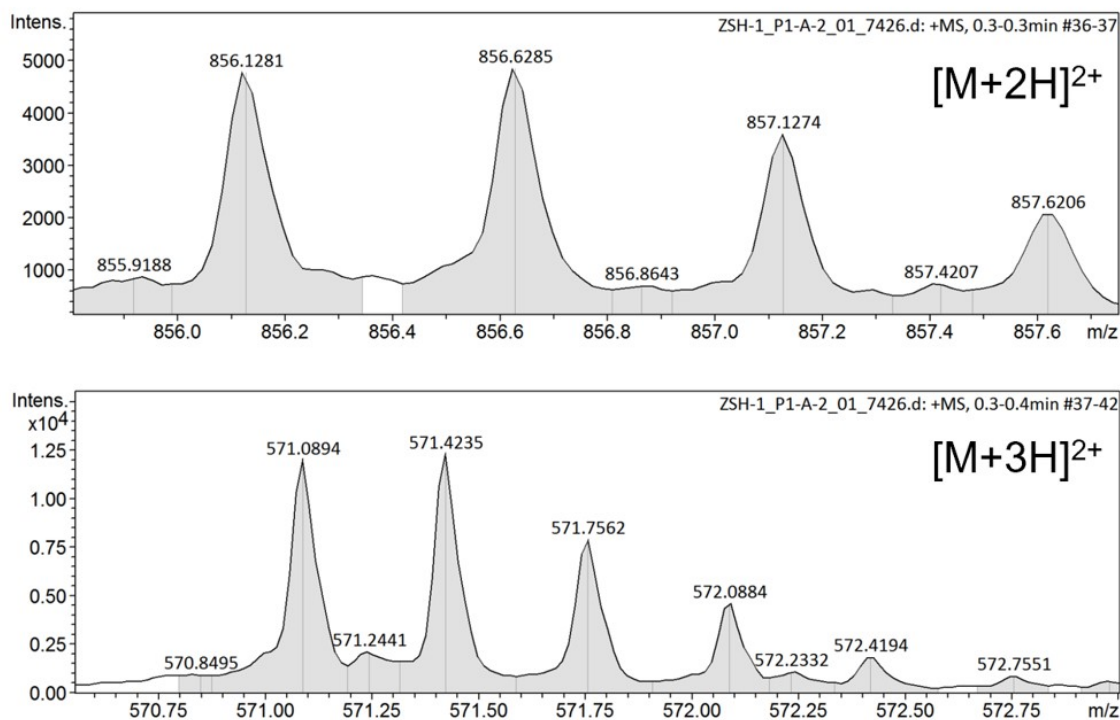
A**B****C**

Fig. S4. HPLC (A), ESI-MS (B) and HRMS (C) analysis of the Pam₃CSK₄-Spacer-OH₂. The synthesis of Pam₃CSK₄-Spacer-OH₂ can be seen in Scheme S3.

1.4 Synthesis of the Pam₃CSK₄-RBD

The Pyridoxal 5'-Phosphate (PLP) and Spike RBD protein were mixed in a 1.5 mL tube to achieve a final concentration of 50 μ M RBD and 10 mM PLP at room temperature in PBS (pH=6.5) for 24 h. In this step, it's worth noting that the pH needs to be carefully adjusted. Then PLP was removed by size-exclusion gel filtration (10 KD, 6000 rpm), the PLP that are not involved in the reaction need to be removed as clean as possible. The keto-RBD and freshly prepared Pam₃CSK₄-Spacer-ONH₂ (50-fold molar excess of keto-RBD) were mixed at room temperature in PBS (pH=5.5) containing 20% DMF for 48 h. Then Pam₃CSK₄-Spacer-ONH₂ was removed by size-exclusion gel filtration (10 KD, 8000 rpm) with 10% DMF in water. Due to the covalent coupling of Pam₃CSK₄, RBD-Pam₃CSK₄ does not dissolve well in pure water. Therefore, the unreacted RBD and RBD-Pam₃CSK₄ can be separated by centrifugal precipitation (1000 rpm) with a small amount of water. Meanwhile, by detecting the concentration of unreacted RBD in the aqueous phase, the total yield can be calculated as over 80%, which is consistent with the previous model reaction.

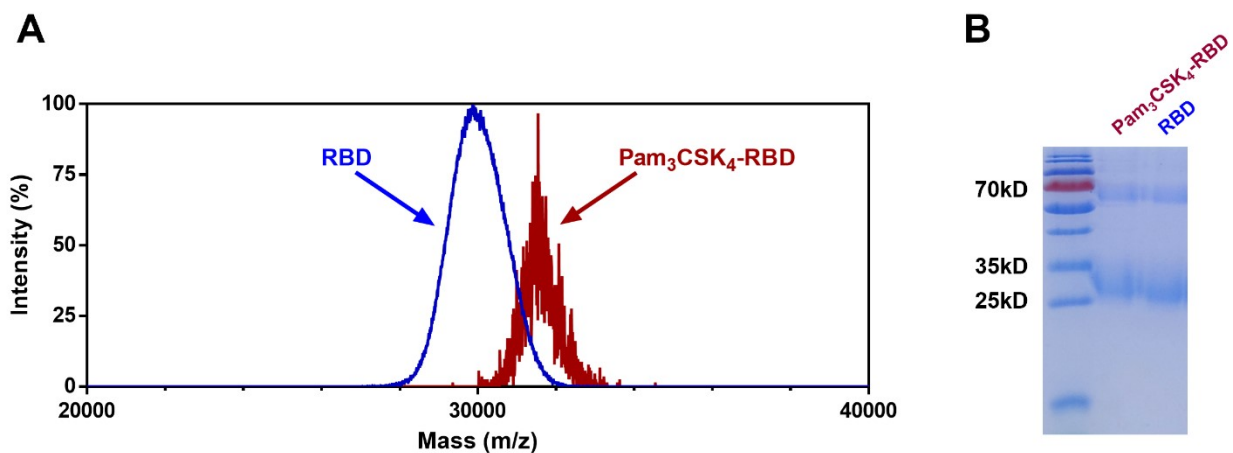


Fig. S5. MALDI-TOF-MS (A) and SDS-PAGE analysis (B) of RBD and Pam₃CSK₄-RBD. Since the molecular weight (MW) difference between RBD and Pam₃CSK₄-RBD is not significant (1.7 kD), only slight shift can be observed in the SDS-PAGE analysis.

2 Evaluation of Vaccine Candidates

2.1 Vaccine formulation

Vaccines	Antigen	Adjuvant	DSPC	Cholesterol
A	RBD (10.0 μ g)			
B	RBD (10.0 μ g)	Alum (100 μ L)		□
C	RBD (10.0 μ g)	Pam ₃ CSK ₄ (0.5 μ g)	11.8 μ g	4.6 μ g
D	Pam ₃ CSK ₄ -RBD (10.5 μ g)		11.8 μ g	4.6 μ g

Table S1. The composition of each vaccine: the amount of each component in the table are used for one injection per mouse.

2.2 Characterization of vaccines

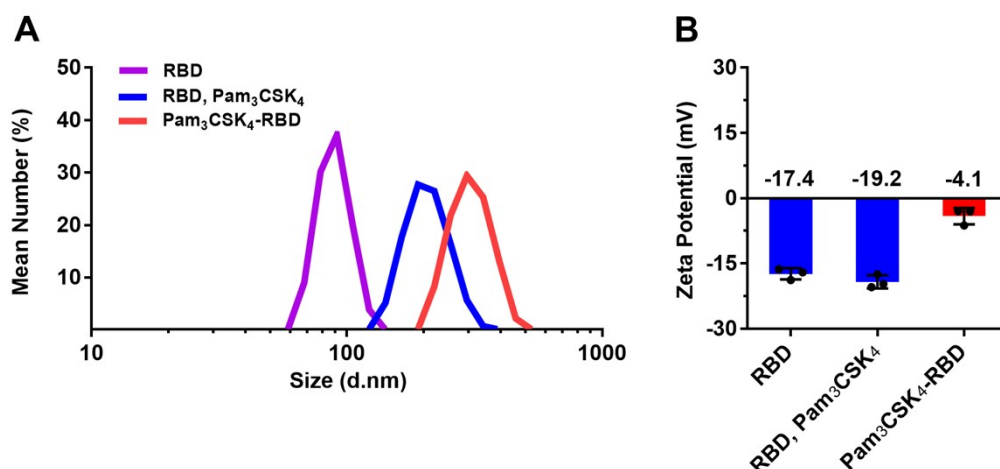


Fig. S6. (A) Dynamic light scattering (DLS) results of vaccines, the mean diameter of RBD, RBD/ Pam₃CSK₄ and Pam₃CSK₄-RBD measured by intensity of volume are 89 nm (PDI=0.699), 208 nm (PDI=0.665) and 309 nm (PDI=0.344), respectively. (B) Zeta potential results of vaccines, values are presented as the mean \pm SD (n=3). DLS and zeta potential were carried out on a Malvern ZEN3600 Zetasizer apparatus.

2.3 Immunological evaluation

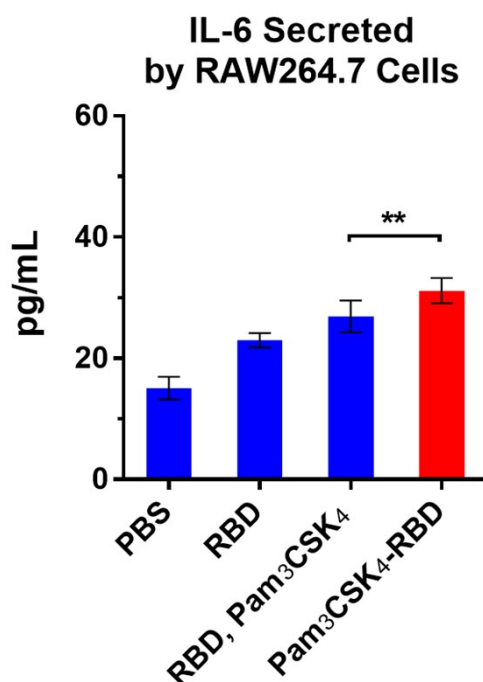


Fig. S7. IL-6 secreted by RAW264.7 cells stimulated by PBS, RBD, RBD/Pam₃CSK₄ and Pam₃CSK₄-RBD for 20 h. The data are expressed as the mean \pm SEM. Asterisks show significant difference based on one-way ANOVA by Dunn's multiple comparison test (no significant difference, ns; $P \leq 0.05$, *; $P \leq 0.01$, **; $P \leq 0.001$, ***; $P \leq 0.0001$, ****). Related to Fig. 2A.

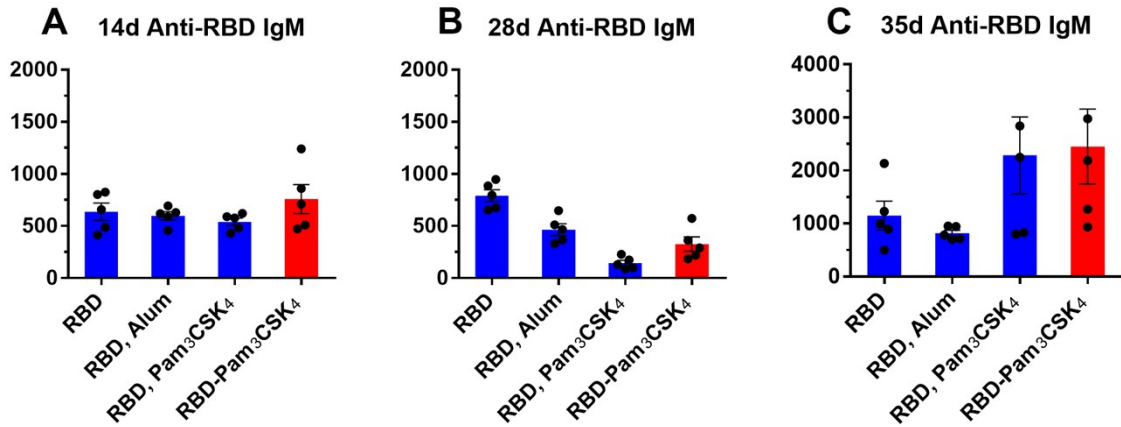


Fig. S8. Anti-RBD IgM responses after subcutaneous injection of mice on days 14, 28 and 35 (A-C). The data are indicated as the mean \pm SEM, individual symbols represent individual mouse titers.

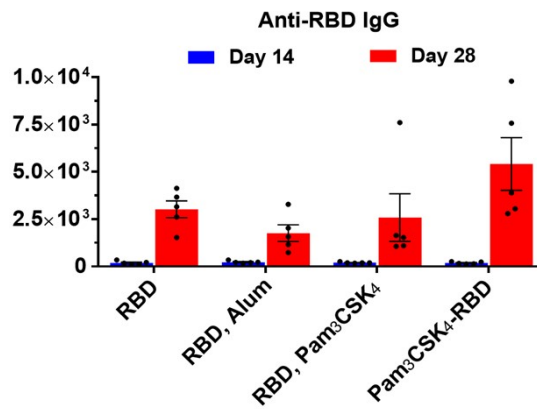


Fig. S9. Anti-RBD IgG responses after subcutaneous injection of mice on days 14 and 28. The data are indicated as the mean \pm SEM, individual symbols represent individual mouse titers.

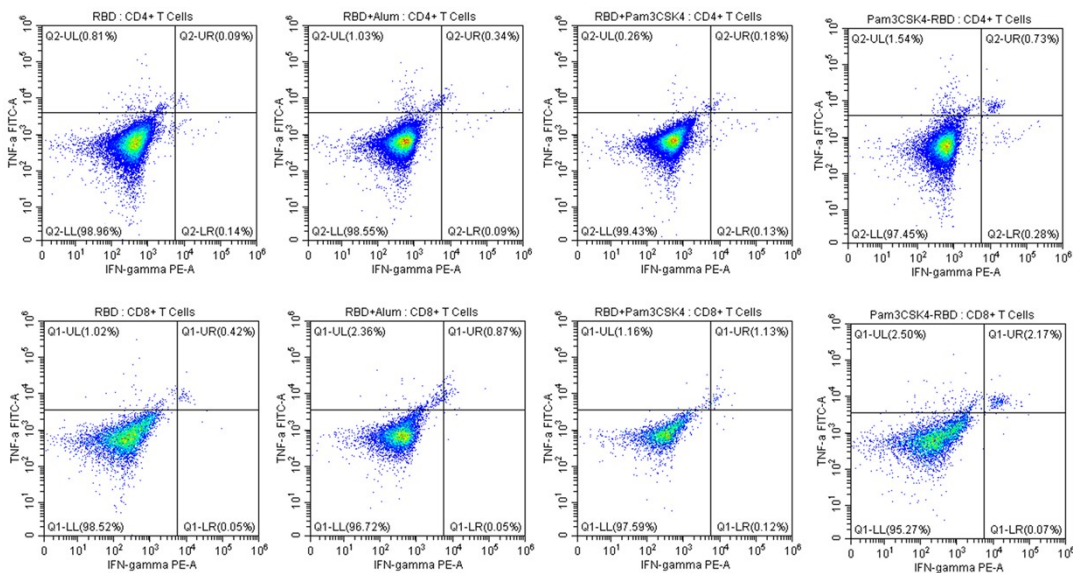


Fig. S10. The lymphocytes in the spleen (day 35) were stimulated with the overlapping peptides for 18h, the results were analyzed by flow cytometry. Representative flow cytometry plots were shown in Fig.. Related to Fig. 4A-D.

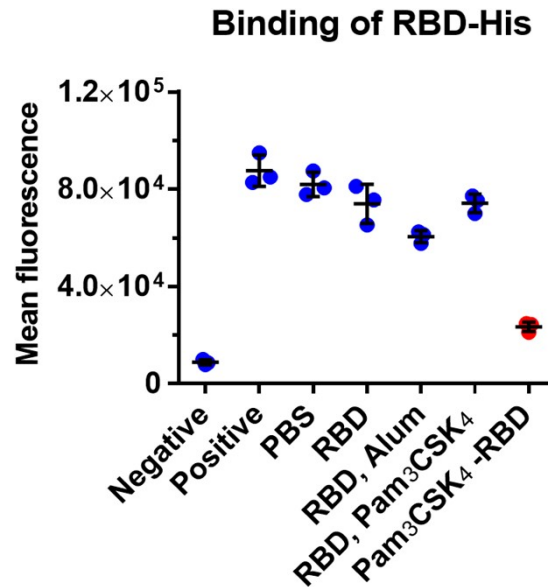


Fig. S11. Mean fluorescence in the flow cytometry analysis. The data are indicated as the mean \pm SD. Related to Fig. 5A.

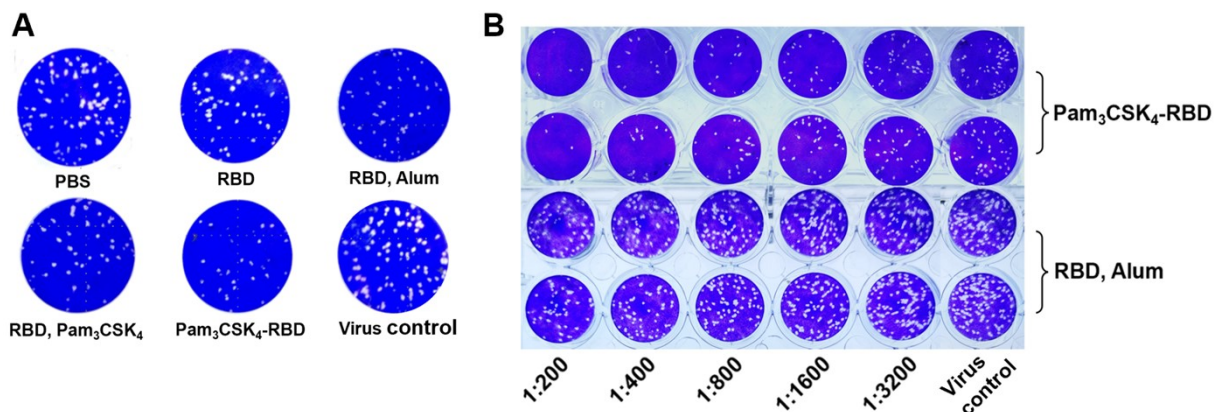


Fig. S12. (A) plaques formed in Vero E6 cells inoculated with live SARS-CoV-2 and 400-fold diluted pooled sera, then inhibition rates were calculated with virus control. Related to Fig. 5E (B) Plaques formed in Vero E6 cells inoculated with live SARS-CoV-2 and sera from Pam₃CSK₄-RBD or alum group. Based on the inhibition curve of the neutralization assay, NT₅₀ was calculated. Related to Fig. 5F.

3 Biological testing methods

3.1 Culture and stimulation of RAW264.7 cells

RAW264.7 cells were maintained in RPMI-1640 supplemented with 10% FBS and 1% antibiotics and kept at 37 °C under a 5% CO₂ atmosphere. For the stimulation of the RAW264.7 cells, cells were seeded in a 24-well culture plate (3×10^5 per well) and incubated with PBS, RBD (10 μ g/well), RBD/Pam₃CSK₄ (10 μ g and 0.5 μ g/well, respectively) and Pam₃CSK₄-RBD (10.5 μ g/well) for 20 h. Then the RAW264.7 cells were incubated with PE Rat anti-mouse CD86 antibody (BD Biosciences, 553692) for 1 h. After washing, cells were analyzed on a

CytoFLEX S flow cytometer (Beckman Coulter). In addition, IL-6 secreted into the culture medium by RAW264.7 cells were measured using Mouse IL-6 ELISA Set (BD Biosciences, 555240). As shown in Fig. S4, the adjuvant-protein conjugate Pam₃CSK₄-RBD also increased the level of IL-6 secretion of RAW264.7 cells after stimulation (15 pg/mL for PBS, 23 pg/mL for RBD, 27 pg/mL for RBD/Pam₃CSK₄ and 31 pg/mL for Pam₃CSK₄-RBD, respectively).

3.2 Immunization of mice and ELISA

Female SPF BALB/c mice aged 6–8 weeks were purchased from Huazhong Agricultural University, mice were randomly divided into 4 groups with 5 mice per cage. The antigens of mice immunized were diluted with PBS. Mice were vaccinated by subcutaneous injection, then mice in each group were injected with the corresponding dosage form of the same dose once every 2 weeks (see Table S1). The sera were collected on days 0, 14, 28 and 35 after inoculation. Mice were euthanized on day 35 after vaccination, the splenocytes were collected and subjected to ELISpot assay and intracellular cytokine staining. Mice used in the vaccination were conducted strictly in accordance with the principles of welfare and ethics of medical laboratory animals. After collection, the blood samples were coagulated at room temperature for 1 h, and centrifuged at 4 °C and 6000 rpm for 8 minutes. The upper sera were stored at -80 °C. For ELISA, 10 µg Spike RBD protein was diluted in 10 mL NaHCO₃ buffer (pH=9.5), then coated on 96-well plates at 100 µL per well overnight at 4 °C. The plates were washed with PBST (PBS with 0.05% Tween-20) 3 times, and then blocked with 3% BSA in PBS at 100 µL per well for 1 h. Subsequently, the gradient diluted sera were added to 96-well plates at 37 °C for 1 h. Plates were washed 3 times and anti-mouse HRP-conjugated antibody diluted with PBS was added into wells for 1 h at 37 °C. Finally, plates were washed 5 times with PBST and color developed with TMB for 5 min at 25 °C, followed by 2 M H₂SO₄ stop solution. The absorptions at OD 450 nm was measured on BioTek SYNERGY H1.

To determine whether the Pam₃CSK₄-RBD conjugate stimulated the production of cytokines in mice, four groups of mice were immunized with PBS, RBD (100 µg/mouse), RBD/Pam₃CSK₄ (100 µg and 5 µg/mouse, respectively) and Pam₃CSK₄-RBD (105 µg/mouse). Sera were collected after 2 h of subcutaneous injection, IL-6 were measured using Mouse IL-6 ELISA Set (BD Biosciences, 555240).

3.3 Enzyme-linked immunospot (ELISpot) assay

The antigen specific T cell responses were detected by ELISpot assays. The splenocytes were isolated 7 days after receiving final vaccination, then the assays were performed using Mouse

IFN- γ precoated ELISpot kit (Dakewe, 2210005). In brief, the splenocytes were seeded at 1×10^6 cells per well and stimulated with Spike-derived overlapping peptides (GenScript, RP30020, 15 mers with 11 aa overlap) *in vitro*. After 18 h, biotinylated antibody and streptavidin-HRP were added into plates, and then the spots were developed by AEC solution at 37 °C for 15 min, finally the spots were counted using ELISpot reader.

3.4 Intracellular cytokine staining (ICS)

Similar to ELISpot assay, mouse splenocytes were stimulated with Spike-derived overlapping peptides, the cells were incubated with brefeldin A and monensin overnight after four hours of stimulation.⁴ After washing, cells were stained with APC/Cyanine7 anti-mouse CD3, PE/Cyanine7 anti-mouse CD4 and APC anti-mouse CD8a (BioLegend) for 30 min, then cells were fixed and permeabilized with PE anti-mouse IFN- γ and FITC anti-mouse TNF- α (BioLegend). Cells were analyzed and gated on a CytoFLEX S flow cytometer (Beckman Coulter).

3.5 Culture of ACE2-HEK293 cells and flow cytometry analysis

ACE2-HEK293 cells were maintained in DMEM supplemented with 10% FBS and 1% antibiotics and kept at 37 °C under a 5% CO₂ atmosphere. For the flow cytometry analysis, sera from five mice were mixed and ACE2-HEK293 cells were added to the 1.5 mL microcentrifuge tube (1×10^6 /tube), recombinant Spike RBD-His protein (GenScript, final concentration of 0.5 μ g/mL) was added to the tubes in the presence or absence of the pooled antisera at 1:10 dilution for 1 h. The group without sera were used as positive control and the group without RBD-His used as negative control.⁵ Cells were washed with PBS and stained with His Tag Antibody iFluor 647 (GenScript, A01802) for 30 min. After washing, cells were analyzed on a CytoFLEX S flow cytometer (Beckman Coulter).

Inhibition rate (%) = $100 - (\text{experimental value} - \text{negative control}) / (\text{positive control} - \text{negative control}) \times 100$

3.6 Pseudovirus and live SARS-CoV-2 neutralization assay

For the pseudovirus neutralization assay, the COVID-19 Spike protein pseudovirus (wild-type, Genomeditech, GM-0220PV07), contains the Spike envelope protein and the luciferase reporter gene. Mouse sera was per-heated at 56 °C for 30 min and then diluted from 100-fold to 3200-fold with complete medium in 96-well plates (Corning, Cat: 3610), then the pseudovirus (2×10^4 TCID₅₀/well) and ACE2-HEK293 (2×10^4 /well) were incubated in the presence or absence

of sera for 48 h. Wells without sera were used as a negative control. Luciferase was detected by Bio-lite Luciferase assay system (Genomeditech, GM-0220PV02-1) and luminescence was measured on BioTek SYNERGY H1. 50% or 90% neutralization titers (pVNT₅₀ or pVNT₉₀) were calculated with 50% or 90% relative luminescence units (RLU) of the virus control. In addition, the VOCs pseudovirus 50% neutralization titers were also tested by the method described above (Genomeditech, GM-0220PV33 for B.1.1.7, GM-0220PV32 for B.1.351, GM-0220PV47 for P.1 and GM-0220PV45 for B.1.617.2).

For the live SARS-CoV-2 Neutralization Assay, Vero E6 cells were seeded in a 24-well culture plate (1.5×10^5 per well) overnight. Sera were inactivated by heat (30 min at 56 °C) and diluted in DMEM with 2% FBS. Then SARS-CoV-2 working stock containing 200 TCID₅₀ was mixed with samples and incubated for 1 h. The cell supernatant of the 24-well culture plate was removed and then the sera-virus mixture was added in the plate at 37 °C for 1 h. The mixture was removed from cells and then the DMEM containing 2% FBS and 0.9% carboxymethyl cellulose was added in the plate. After three days, Vero E6 cells were fixed and stained. Inhibitions and NT₅₀ were calculated according to the positive control (without sera).^[6] All the live SARS-CoV-2 Neutralization Assay were performed at Wuhan Institute of Virology.

3.7 Statistical analysis and references

Data in the Fig.s were analyzed using GraphPad Prism 6. Except as specifically stated, all values were mean and error bars were SEM. Significance of groups in comparison was analyzed using one-way ANOVA by Dunn's multiple comparison test. Asterisks showed significant difference (no significant difference, ns; $P \leq 0.05$, *; $P \leq 0.01$, **; $P \leq 0.001$, ***; $P \leq 0.0001$, ****).

References

1. J. J. Du, S. Y. Zou, X. Z. Chen, W. B. Xu, C. W. Wang, L. Zhang, Y. K. Tang, S. H. Zhou, J. Wang, X. G. Yin, X. F. Gao, Z. Liu and J. Guo, *Chem - An Asian J*, 2019, **14**, 2116–2121.
2. X. Z. Chen, R. Y. Zhang, X. F. Wang, X. G. Yin, J. Wang, Y. C. Wang, X. Liu, J. J. Du, Z. Liu and J. Guo, *Mol Pharm*, 2019, **16**, 1467–1476.
3. J. Shi, D. Zhao, X. Li, F. Ding, X. Tang, N. Liu, H. Huang and C. Liu, *Org Biomol Chem*, 2020, **18**, 6829–6839.
4. M. P. Steinbuck, L. M. Seenappa, A. Jakubowski, L. K. McNeil, C. M. Haqq and P. C. DeMuth, *Sci Adv*, 2021, **7**, 5819.
5. X. Qi, B. Ke, Q. Feng, D. Yang, Q. Lian, Z. Li, L. Lu, C. Ke, Z. Liu and G. Liao, *Chem Commun*, 2020, **56**, 8683–8686.
6. J. Gai, L. Ma, G. Li, M. Zhu, P. Qiao, X. Li, H. Zhang, Y. Zhang, Y. Chen, W. Ji, H. Zhang, H. Cao, X. Li, R. Gong and Y. Wan, *MedComm*, 2021, **2**, 101–113.

